Hindawi
Advances in High Energy Physics
Volume 2021, Article ID 6672655, 10 pages
https://doi.org/10.1155/2021/6672655

Research Article

Feasibility Study of an Alcohol-Based Liquid Scintillation Detector and Its Application

Byoung Chan Kim,[1,2] **Ji Young Choi**,[2] **Kyung Kwang Joo**,[2] **Seon Yeong Park**,[2] **Ye Sung Song**,[2] **and Hee Jin Woo**[2]

[1]*Department of Radiation Oncology, Chonnam National University Hwasun Hospital, Seoyang-ro 322, Hwasun-eup, Hwasun-gun, Jeollanam-do, Republic of Korea 58128*
[2]*Institute for Universe & Elementary Particles, Department of Physics, Chonnam National University, Yongbong-ro 77, Buk-gu, Gwangju, Republic of Korea 61186*

Correspondence should be addressed to Ji Young Choi; opercjy@gmail.com and Kyung Kwang Joo; kkjoo@chonnam.ac.kr

Received 30 October 2020; Revised 24 February 2021; Accepted 27 March 2021; Published 16 April 2021

Academic Editor: Xiaochun He

This paper proposes a new base material, a mixture of alcohol and water, for liquid scintillators. A possibility of using alcohol as a new detection solution in a particle detector is described. A liquid scintillator is widely used in various fields because of its high light yield. In addition, it is very important to develop a stable liquid scintillator for particle detectors or other medical applications. To date, there have been no previous R&D studies elsewhere for the use of alcohol in particle detectors, and no market products are available of this type. Thus, there is a room for improvement. This paper describes the brief synthesizing process of the alcohol-based liquid scintillator by varying the mixing ratio of each component that makes up the liquid scintillator. The several feasible physical and optical properties of an alcohol-based liquid scintillator were investigated and presented. Finally, as one of its applications, a range (beam-path length) measurement using an electron beam in medical physics is introduced after irradiating an alcohol-based liquid scintillator with electron beam energies of 6~12 MeV. The measurement results were compared with a Monte Carlo simulation, Novalis Tx, a phantom, and a CT image. In the near future, the new alcohol-based liquid scintillator could be used for particle detector or medical imaging applications.

1. Introduction

A liquid scintillator (LS) is widely used in nuclear, particle, and medical physics [1–5]. In general, the liquid scintillator contains a mixture of an organic base solvent and fluor. A solvent has aromatic rings and absorbs the energy of incident particles. The energy passes back and forth among the solvent systems, allowing efficient capture by dissolved fluors. The purpose of a primary fluor is to pick up excitation energy from the solvent and emit some fraction of this energy as light. Most primary fluors emit light in the ultraviolet (UV) range with wavelengths shorter than 400 nm. In addition, a secondary wavelength shifter (WLS) is sometimes added in order to shift the wavelength to the sensitive region of the photomultiplier tube (PMT). The emitted fluorescence light is detected by a PMT. Typically, a PMT bialkali photocathode has a maximum quantum efficiency (QE) at wavelengths around 400~430 nm. The more light emitted by the LS, the greater the size of the pulse produced by the PMT. In addition, in order for the light to reach the PMT, the LS should have as few impurities as possible and excellent physical and optical properties.

Since benzene (C_6H_6) was being used as the basic solvent for LS in the 1950s, dioxane ($C_4H_8O_2$), toluene (C_7H_8), and xylene (Cylene, C_8H_{10}) have all been developed. Subsequently, a pseudocumene- (PC-, C_9H_{12}) based LS developed in the 1970s has been used for a long time due to its excellent light emission. However, PC has a benzene ring and a low flashing point (~45°C). Since the 1980s, many attempts have been made to replace it due to potential hazards to humans and the environment. To make more modern biodegradable and disposable solvents, phenylxylylethane (PXE, $C_{16}H_{18}$),

diisopropylnaphthalene (DIN, $C_{16}H_{20}$), and linear alkyl benzene (LAB, C_nH_{2n+1}-C_6H_5, $n = 10 - 13$) were developed in the early 1980s. These are what are used as the base solvent in reactor neutrino experiments and next-generation neutrino experiments [6, 7]. As a fluor, 2,5-diphenyloxazole ($C_{15}H_{11}NO$, PPO) is frequently used. For a secondary WLS, 1,4-bis(5-phenyl-2-oxazolyl)benzene ($C_{24}H_{16}N_2O_2$, POPOP) and 1,4-bis(2-methylstyryl)benzene ($C_{24}H_{22}$, bis-MSB) can be added.

2. Motivation

This study focuses on using alcohol as a method of dissolving fluors without using a surfactant in the process of developing a water-based LS that can be mixed with water and oil. One of the alcohols studied, ethanol (C_2H_5OH), is called ethyl alcohol. This type of alcohol has a characteristic odor, and a flammable compound is one of the main components. The steam of alcohol is explosive, and this is often industrially used as a solvent, disinfectant, and fuel. It exists as a colorless liquid at room temperature. The melting point is -114.5°C, the boiling point is 78.32°C, the molar mass is 46.07 g/mol, and the density is 0.789 g/cm^3. The flash point is 16.6°C when in contact with an external flame, and the ignition point is 365°C in its natural state. Fluors are relatively well soluble in alcohol; in addition, alcohol and water can also be well mixed with each other. Therefore, after the fluor is dissolved in alcohol and diluted with water, we expect that if the alcohol is slowly evaporated, there would be only the fluor in the water without the use of a surfactant. However, the results achieved are completely different depending on the mixing ratio of alcohol and water.

On the other hand, when performing radiation-related experiments on the human body in the field of medical physics, dilution of alcohol with water is used to make an equivalent substance to human material such as the skin. Therefore, the possibility of using alcohol as a solvent in LS has been investigated. However, the density of this kind of LS is still rather low for human materials; also, secondary WLS does not dissolve well in this mixture. As such, in this study, 2-ethoxyethanol ($C_4H_{10}O_2$, ethylene glycol ethyl ether (EGEE)) was used to make an LS with a density similar to that of the human body and to dissolve fluor and secondary WLS. 2-Ethoxyethanol is transparent and colorless, has a boiling point of 135°C, a flash point of 44°C, a molar mass of 90.12 g/mol, and a density of 0.930 g/cm^3. It mixes well with water, alcohol, acetone, etc. It is widely used for biological, chemical, and research purposes because it also dissolves oil, resin, grease, and wax. In addition, since it is diluted with water, safety concerns due to the risk of vapor pressure and a low flash point, which are a common disadvantage of alcohol, are reduced. In addition, by dissolving the fluor and secondary WLS, the density can be further increased. Also, by diversifying the LS components, it can be made more similar to the desired human body component.

There has been no study where alcohol-based LS is directly synthesized and used with detectors or in medical physics; as such, there are no R&D results for this kind of experiment. In medical physics, it is used in dosimetry systems [8]. In general, a plastic scintillator is expensive and has the disadvantage in that it cannot be used for a long time, because it becomes contaminated and colored when exposed to a large amount of radiation. However, LS is relatively inexpensive and easy to replace. By varying the mixing ratio of the components constituting the LS, its physical and optical properties, light yield, and range ("beam-path length") can be easily controlled.

In addition, as an example of the use of an alcohol-based LS, we measured its "range" by irradiation with an electron beam. A range means the average distance that charged particles can penetrate through a substance. Electron beams have been used in medical physics for more than 20 years. This is a significant improvement over treatment with only X-rays. With the installation of high-energy linear accelerators, the use of electron beam therapy is currently increasing. Irradiation damages both normal and cancer tissues but causes more fatal damage to cancer tissues due to much faster cell fission. Since normal tissues recover over time, medical physics is now applying the method of irradiating small doses of electron beams at the target area several times, avoiding damage to vital body organs.

Medical physics covers a large field of science. Therefore, one of the aims of this study is to research methods for using alcohol-based LS during irradiation of electron beams in the treatment of tumors or cancers occurring over a small area of the skin surface or epidermis. To this end, reconstruction was carried out through a Monte Carlo (MC) simulation, and the computational simulation related to detection was performed using Geant4 software. Then, the MC results were compared with Novalis Tx, phantom, and computed tomography (CT) analysis results that are used in cancer treatment.

3. Alcohol-Based Liquid Scintillator and Results

3.1. Sample Synthesis and Optical Property Measurement. In general, the amount of optimized fluor in organic LS used in high-energy physics is approximately ~3 g/l, and WLS is ~30 mg/l [1, 2, 4]. PPO dissolves very well in alcohol (99.9% purity). Here, ultrapure water is dropped at a speed of one drop per second, diluting the solution using a stirrer while mixing with a magnet bar with 20 rpm. Up to a 1 : 1 mixing ratio of alcohol and ultrapure water can be mixed in several minutes without any major problems and remains transparent. If water does not dissolve, we can mix it for a longer time, or we can increase the heating temperature to about 30°C. In this case, it is very important to pay attention to laboratory safety. However, when the proportion of ultrapure water is higher than that of alcohol, the liquid becomes opaque, and precipitation of fluor and secondary WLS begins to occur at the bottom. All samples we synthesized are listed in Table 1. It summarizes the ratio of alcohol and ultrapure water, as well as the contents of fluor and secondary WLS. The difference between the S sample and the NE sample is the use of alcohol and 2-ethoxyethanol. The reference (R) sample consists of a mixture of LAB and commercially available DIN (Ultima Gold F, UG-F). PPO was dissolved at 3 g/l in LAB, and 30 mg/l bis-MSB was mixed as the secondary WLS, while gadolinium (Gd) was loaded at 0.5%

Table 1: Samples used for synthesizing alcohol-based liquid scintillator. In the standard sample (R), used as a reference, 3 g/l PPO was dissolved and 30 mg/l bis-MSB was mixed as the second WLS in the LAB and UG-F. The S samples indicate alcohol-based LS and NE samples based on 2-ethoxyethanol solvent.

Sample	Composition of solvent (%)	Fluor, secondary WLS	Note
S1	Alcohol : water (50 : 50)	PPO 6 g/l	Clear, soluble (marginal)
S2	Alcohol : water (70 : 30)	PPO 21 g/l	Clear, soluble
S3	Alcohol : water (70 : 30)	PPO 30 g/l, bis-MSB 300 mg/l	Insoluble
S4	Alcohol : UG-F (70 : 30)	PPO 3 g/l, POPOP 30 mg/l	Clear, soluble
S5	Alcohol : UG-F (70 : 30)	PPO 3 g/l, bis-MSB 30 mg/l	Clear, soluble
NE0	2-Ethoxyethanol : UG-F (70 : 30)	PPO 3 g/l, bis-MSB 30 mg/l	Clear, soluble
NE1	2-Ethoxyethanol : UG-F (30 : 70)	PPO 3 g/l, bis-MSB 30 mg/l	For PSD check
NE2	2-Ethoxyethanol : water (100 : 0)	PPO 15 g/l, bis-MSB 300 mg/l	Clear, soluble (bis-MSB extreme)
NE3	2-Ethoxyethanol : water (90 : 10)	PPO 15 g/l, bis-MSB 60 mg/l	Clear, soluble
NE4	2-Ethoxyethanol : water (70 : 30)	PPO 21 g/l	Clear, soluble
NE5	2-Ethoxyethanol : water (70 : 30)	PPO 21 g/l, bis-MSB 120 mg/l	Insoluble
NE6	2-Ethoxyethanol : water (50 : 50)	PPO 1 g/l	Clear, soluble
NE7	2-Ethoxyethanol : water (30 : 70)	PPO 1 g/l	Clear, soluble
NE8	2-Ethoxyethanol : water (20 : 80)	PPO 1 g/l	Clear, soluble
NE9	2-Ethoxyethanol : water (10 : 90)	PPO 1 g/l	Insoluble
NE10	2-Ethoxyethanol : water (10 : 90)	PPO 0.5 g/l	Insoluble
NE11	2-Ethoxyethanol : water (10 : 90)	PPO 0.3 g/l	Insoluble (first clear, but precipitate in the end)
NE12	2-Ethoxyethanol : water (10 : 90)	PPO 0.2 g/l	Barely soluble
NE13	2-Ethoxyethanol : water (10 : 90)	PPO 0.2 g/l, bis-MSB 20 mg/l	Clear, soluble (marginal)
NE14	2-Ethoxyethanol : water (10 : 90)	PPO 0.1 g/l, bis-MSB 10 mg/l	Clear, soluble
R	LAB : UG-F (90 : 10)	PPO 3 g/l, bis-MSB 30 mg/l	0.5% Gd (clear, soluble) Reference sample

concentration. This reference sample is commonly used in reactor neutrino experiments [5, 9, 10].

In the case of alcohol sold at pharmacies and used for hygiene, water is already mixed in and makes up approximately 30%. On the other hand, when the amount of alcohol is ~2 times more than ultrapure water, fluor can be dissolved up to ~7 times more compared to optimized LS. The water used here was 18 MΩ ultrapure water produced by the Millipore Milli-Q ultrapure system. However, for the secondary WLS, some substances, such as POPOP or bis-MSB, have the disadvantage of not being soluble in ethanol or methanol (CH_3OH). Therefore, 2-ethoxyethanol was used; its density is not much different from that of the human body. It has both hydrophilic and hydrophobic properties. When the ratio of alcohol is high, the LS can be applied in medical physics, and when the ratio of water is high, the LS can be used as a particle detector with Cherenkov light. When dissolving the fluor, the order should be considered. Since PPO or bis-MSB is relatively soluble in 2-ethoxyethanol, it is better to first dissolve these and then dilute with ultrapure water. In general, the solubility of bis-MSB is better than that of POPOP. However, after being mixed for a long time, there is no significant difference between the two. Figure 1 shows a photograph of the prepared LS under illumination from a 250 nm UV lamp. The alcohol-based LS has a light yield that is not significantly different compared to the reference sample alongside.

Figure 1: Light is emitted from samples illuminated by a 250 nm wavelength UV lamp for eye inspection. From left to right, pure water (H_2O), 2-ethoxyethanol, NE3, and R sample. Pure water and 2-ethoxyethanol do not emit light. Our main NE3 sample emits a relatively moderate amount of light compared with the R sample at the rightmost vial in the figure.

In order to use an alcohol-based LS in a high energy particle detector or in medical physics, the emitted light must reach the PMT. The transmittance ([T]) value was measured to find the optical transparency value of our LS. For this, a Shimadzu UV/Vis-1800 spectrophotometer was used, and scans from 200 nm to 700 nm in 1 nm increments were carried out. Absorption (Abs) is calculated by an empirical formula, $\text{Abs} = -\log_{10}(I/I_o)$, where I_o represents the intensity of the incident light and I represents the intensity of the emitted light. Figure 2 shows the transmittance value as a function of the wavelength. The PPO fluor emits light of ~360 nm, and

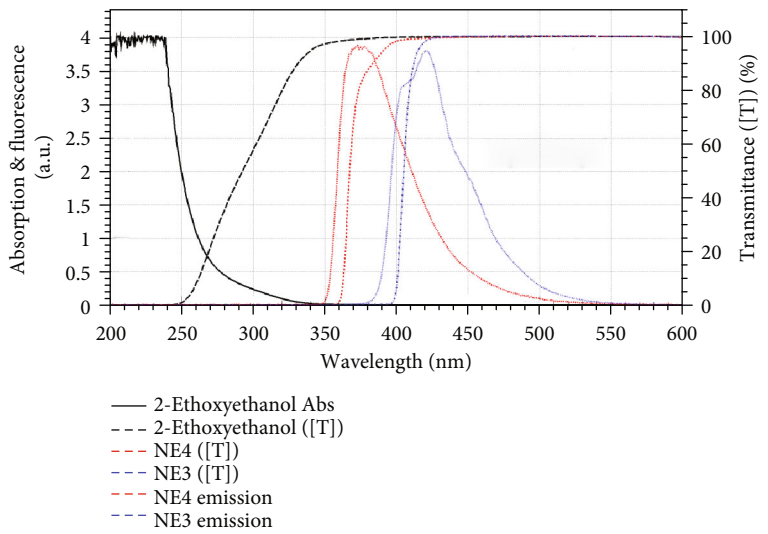

Figure 2: Absorption and emission spectrum as a function of wavelength on one plot. Based on the absorption spectra of the samples, an excitation wavelength was selected. The overlap of absorption and emission spectra in each sample group can be seen.

the secondary WLS bis-MSB absorbs light of this wavelength and emits it at ~420 nm, which then reaches the PMT. The addition of the PPO and bis-MSB continues to shift the wavelength to the right. All measured samples have very high transmittance values of over 97% in the visible region. Figure 2 also shows the energy absorption and emission transfer process between samples. To measure the fluorescence spectrum, a Varian Cary Eclipse fluorescence spectrometer was used. An appropriate excitation wavelength was selected according to the absorption of each sample. Fluorescence values were measured between 300 and 550 nm.

3.2. Alcohol-Based LS Response Measurement

3.2.1. Light Yield. Physical and optical properties of the alcohol-based LS are important, but achieving sufficient light yield is essential for their use in particle detectors [11, 12]. To find the light yield property, a simple data acquisition (DAQ) system was used. A schematic view of the DAQ system can be found in Figure 3. The container was filled with sample, which was then attached to a 2-inch Hamamatsu H7195 PMT, and a source was used. The used PMT was made of bialkali and had a QE of ~23% at a wavelength of 420 nm. For the data processing, a 400 MHz parallel analog-to-digital converter (FADC) capable of measuring pulses every 2.5 ns was used. The FADC DAQ was connected to a Linux system, and finally, the data was collected and analyzed using the C programming language and ROOT.

Among the samples prepared in Table 1, NE3 sample was mainly investigated because it fully reflects our purpose of not using any surfactants as described in our motivation. PPO and bis-MSB can be dissolved in the proportions we need. Furthermore, the ratio of alcohol and water is also suitable, and this ratio can be easily adjusted. Other samples are slight variations of the NE3 sample. Therefore, if the NE3 sample is successful, other samples can be synthesized. To perform a more detailed inspection, the energy spectrum was determined using a ^{137}Cs (0.662 MeV) source in a dark box setup drawn in Figure 3. The position of the peak from the Compton backscattering is used to measure the light yield of the sample. When the light yield of the reference sample (R) was 100, the alcohol-based sample S5 obtained a light yield of about 40% and the 2-ethoxyethanol-based NE4 sample achieved about 50%. In general, the light yield of the sample S5 mixed with bis-MSB showed a more pronounced Compton curve than the POPOP sample S4. NE3 is a sample in which both the PPO and bis-MSB are mixed and shows a light yield of about 60%. The light yield of NE3 can be further improved by controlling the amount of PPO and bis-MSB. Basically, in the sample with a higher ratio of ethanol than water, like NE3, the light yield differs depending on the amount of PPO and bis-MSB, but scintillating light can clearly be seen. On the other hand, even in a sample with more water than alcohol like NE13, it is possible to induce minimal light emission by controlling the amount of the fluor. This is a meaningful result demonstrating the potential to replace the disadvantages of conventional water-based LS using surfactants.

3.2.2. Measurement of Pulse Shape Discrimination. When a LS is used as a particle detector, it is very good to have the ability to discriminate between γ-rays and neutrons. When a particle is passing through the LS, the energy loss of that particle is different according to the type of particle. Therefore, it is possible to distinguish between a fast neutron event and a γ-ray event by obtaining the ratio between the total charge (Q_{total}) and the tail charge (Q_{tail}) of the pulse. As a result, the pulse shape discrimination (PSD) method is now widely used for n/γ discrimination. The quality of PSD can be expressed in a quantitative way in terms of the figure of merit (FoM) as follows [13, 14]:

$$\text{FoM} = \frac{\Delta S}{\sqrt{\sigma_x^2 + \sigma_y^2}}, \tag{1}$$

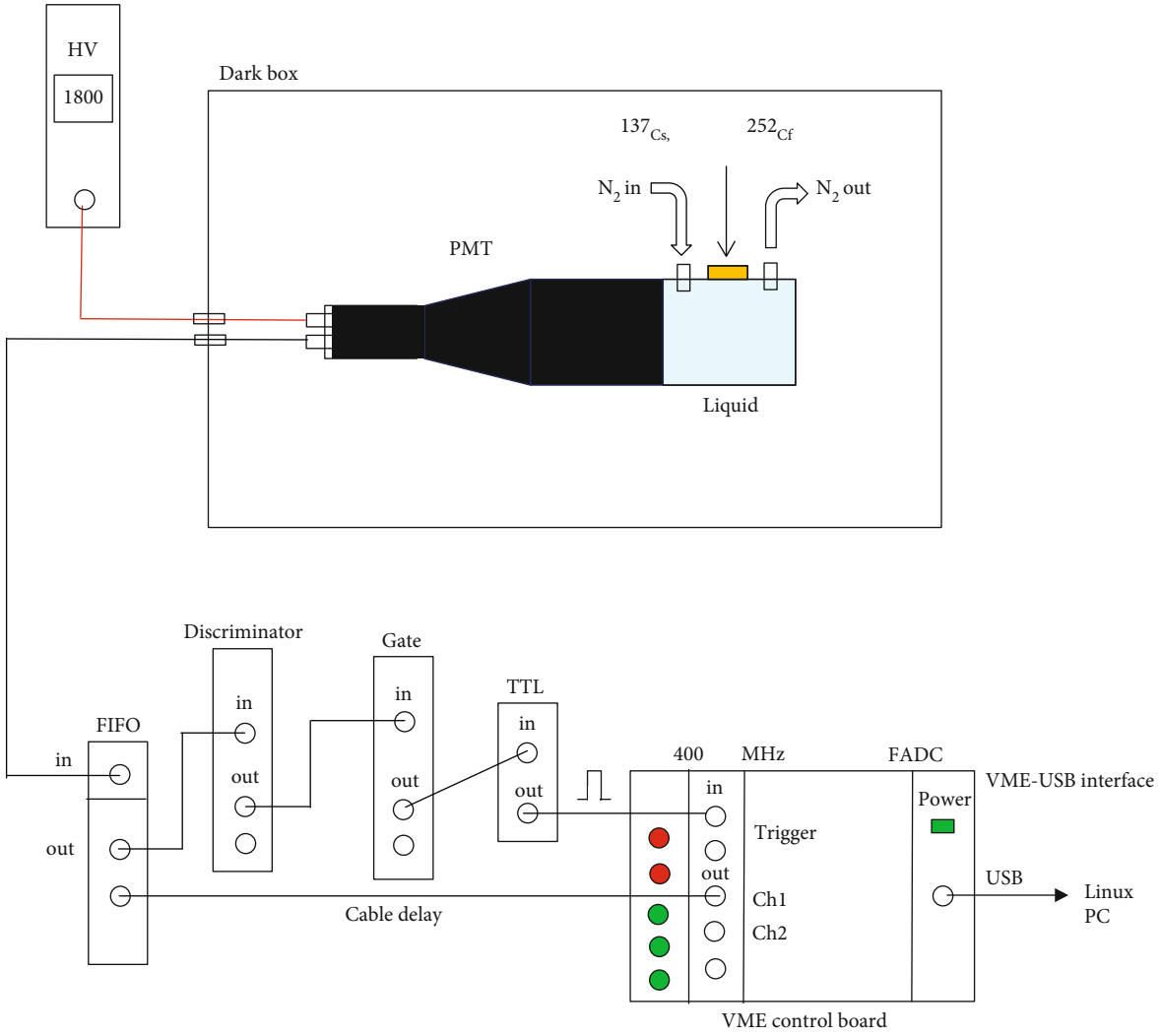

Figure 3: Schematic view of the DAQ system including a 400 MHz FADC readout for light yield and PSD measurement.

where ΔS represents the distance between the peak centroids of the two distributions and σ_x and σ_y are their respective standard deviations. This represents the statistical distance of the two pulse distributions with respect to their separation. The higher FoM value represents better discrimination of the two adjacent spectra. PSD was measured by using a ^{252}Cf source that emits both γ-rays and fast neutrons with a mean energy of 2.14 MeV. Figure 4 shows a scatter plot of $Q_{\text{tail}}/Q_{\text{total}}$ in our samples (NE1, NE3) as a function of energy. The FoM power of the NE1 and NE3 samples are 2.44 and 1.54, respectively. Figure 4(a) shows that neutrons and gammas can be distinguished at a large Q_{total} in the NE1 sample. Mixing UG-F in alcohol provides the ability to distinguish particles. But it is hard to separate between the neutrons and γ-rays in the NE3 case, as shown in Figure 4(b). Figures 4(c) and 4(d) show the number of entries as a function of the $Q_{\text{tail}}/Q_{\text{total}}$ value used to calculate the FoM.

3.3. Medical Applications

3.3.1. Monte Carlo (MC) Simulation Setup. As an example of using alcohol-based LS, the possibility of use in medical physics was investigated. Clinically, the energy range of useful electron beams is from 6 to 20 MeV. In this energy region, electron beams characteristically lose energy within about 5 cm of the skin surface. Therefore, this provides suitable characteristics that can be effectively used to treat surface tumors while minimizing damage to deep tissue [15, 16].

For comparison with electron beam measurements used in radiation oncology therapy, MC simulations were performed. A rectangular container made of acrylic, 5 cm width × 10 cm length × 10 cm height, was designed. The upper side is an open space where electron beams can collide directly; both side surfaces were made of quartz with good optical transmission so that the electron beam can pass through. Specifically, it is assumed that the electron beam is directly incident for the treatment of tumors on the skin surface. The alcohol-based LS was poured into a 0.4 l measuring container. In addition, during the actual radiation therapy, the electron beam was irradiated to a region with a skin radius of about 1 to 1.5 cm and a limited, shallow depth; this was so that the generation point of the electron beam incident from the Geant4 computer simulation could be changed without fixing the generation points. Three types of incident

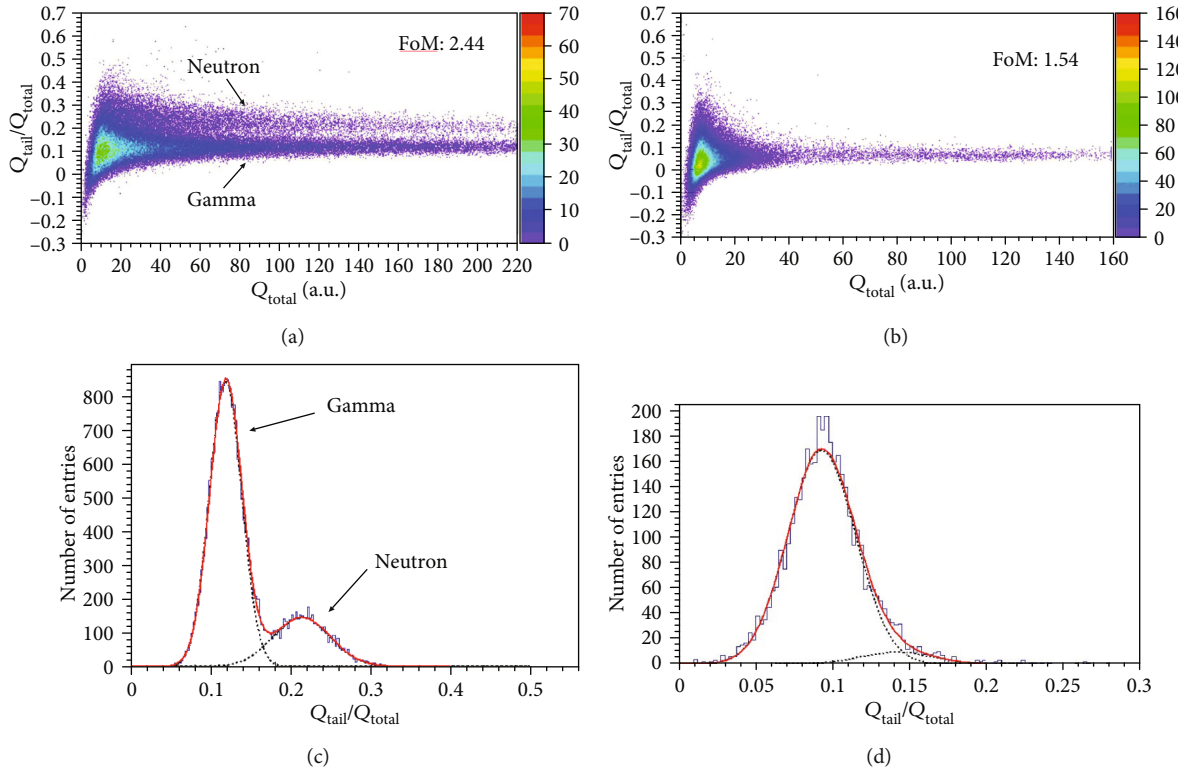

FIGURE 4: Q_{tail}/Q_{total} value of the samples (a) NE1 and (b) NE3 using the PSD method as a function of energy. The Q_{tail} and HV values were varied to optimize the FoM. The NE1 sample enables a relative discrimination of neutron (n) and γ-ray signals. It is hard to separate between the neutrons and γ-rays in the NE3 cases. (c, d) The number of entries as a function of Q_{tail}/Q_{total} value used to calculate the FoM is shown and is fitted by Gaussian function.

energy were generated: 6, 9, and 12 MeV. Furthermore, since the density of the sample used in the range measurement is one of the most important factors, their density needed to be measured with relatively high precision. For this purpose, a portable density meter (DA-130N, KEM) with a resolution of 0.001 g/cm^3 at 0~40°C was used. The density of NE3 at 28°C was 0.945 ± 0.001 (g/cm^3).

3.3.2. Measurement of Beam-Path Length with MC. Figure 5 shows the trajectory of the electron beam traveling into the container when 12 MeV electron beams are injected into a container filled with three different solvents (alcohol, 2-ethoxyethanol, and ultrapure water) with differing densities. The smaller the density, the longer the range. As we noted, the range of electron beams is not a concept defined with a high precision. In the field of radiation therapy, the most commonly used range is the practical range (R_p). The practical range is customarily defined by extrapolating the linear portion of the depth dose curve and the Bremsstrahlung tail. The practical range is selected as the point at which these two lines intersect. Bremsstrahlung accounts for around ~10% of the dose from the electron beam. In the ultrapure water case, R_p is empirically about $E/2$ (cm) [17, 18]. Based on our MC simulation result for the NE3 sample, the practical range is 3.1, 4.7, and 6.3 cm when the incident energy of the electron beam is 6, 9, and 12 MeV, respectively, as shown in Figure 6.

3.3.3. Novalis Tx Result. To compare the MC results of the alcohol-based LS, a range of electron beams were experimentally measured using the Varian Novalis Tx system. Novalis Tx is a radiosurgery system used for tumor and cancer therapy that uses a linear accelerator and scanning electron beams from any angle. Electron beams with energies of 6, 9, and 12 MeV can be produced. Figure 7(a) shows the NE3 sample in a rectangular acrylic container for its range measurement; Figures 7(b)–7(d) shows images taken by a digital camera after 5 seconds of exposure when a 6, 9, and 12 MeV electron beam was irradiating the NE3 sample. The photographed image shows the distribution of a typical electron beam. We measured the distance the electron beam descended from the top of the container. The photographed images are stored in trichromatic values (RGB). Once the RGB values are known, they can be converted to Hue, Saturation, Value (HSV). Only pixels with more than about 20% of brightness (V) value are selected and used to estimate a practical range. When the incident energy of the electron beam was 6, 9, and 12 MeV, the measured distance values were approximately 3.2, 5.0, and 6.5 cm, respectively. The difference between the predicted MC R_p value and the measured distance value is not so large.

3.3.4. Phantom Result. For verification through another method, the phantom technique widely used in radiation dose measurement was applied. A phantom is a useful

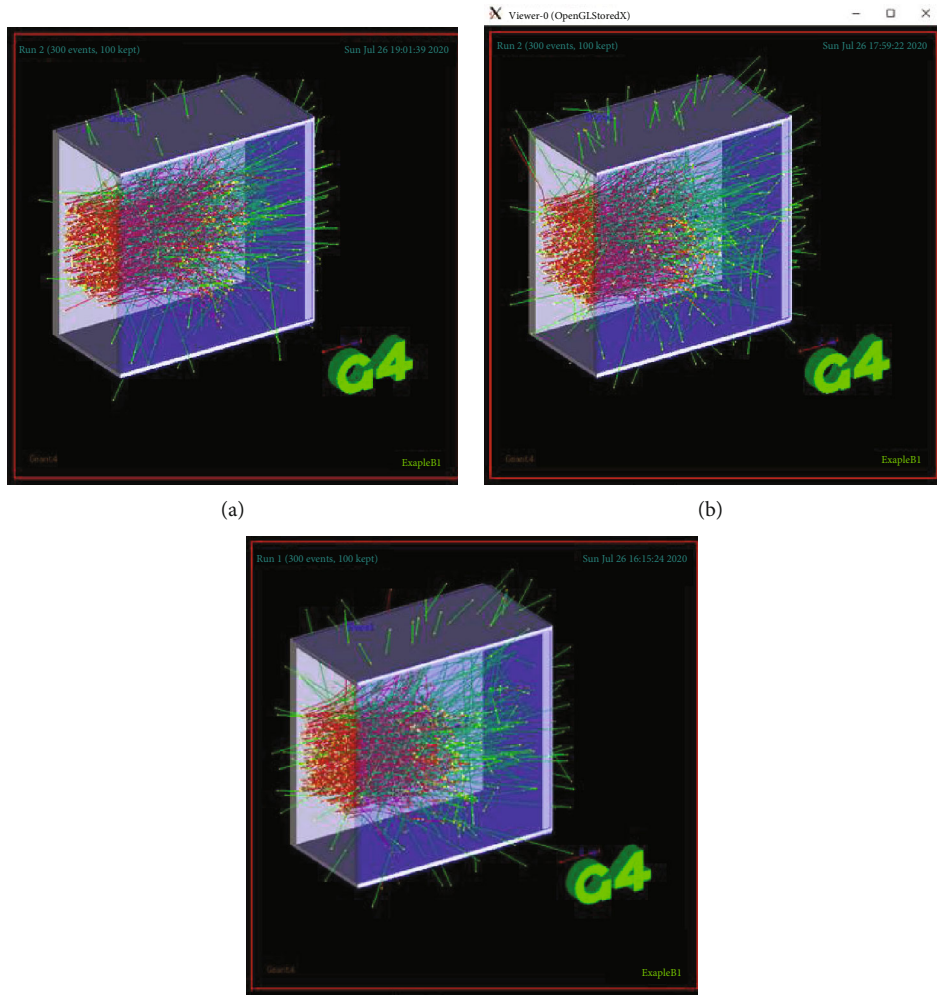

FIGURE 5: Event display of beam-path length of 12 MeV electron beam in acrylic container filled with different densities of solution: (a) 0.78 g/cm^3 (alcohol), (b) 0.93 g/cm^3 (2-ethoxyethanol), and (c) 1 g/cm^3 (pure water). Red color represents electron tracks and green color indicates gamma rays.

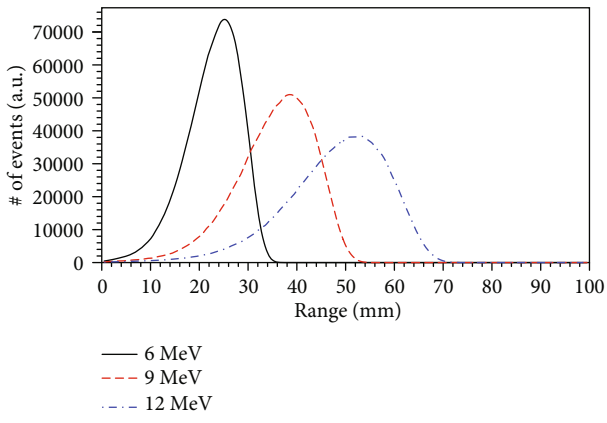

FIGURE 6: A comparison of range using various electron beam energies of 6, 9, and 12 MeV. The practical range (R_p) was measured for each energy.

scientific tool to ensure that systems and methods for medical imaging the human body are operating correctly. It shows how human tissues and organs would respond. Figure 8 shows the range when a 12 MeV electron beam is incident using a phantom (MapPHAN Phantom) used to measure radiation dose. The most important factors in determining range measurement from a phantom are the effective atomic number and density. The phantom density of 1.0 g/cm^3 was used similar to that of the human body. The practical ranges were obtained using the same technique applied in Figure 7. When the electron beams of 6, 9, and 12 MeV were irradiated, it was found that the range in the phantom was 3, 4.5, and 5.7 cm, respectively. The difference between the predicted MC practical range value and the practical range in the phantom is small, when considering the density difference between the MC and the phantom.

3.3.5. CT Image and Novalis Tx Result. For a final crosscheck, after taking an image of the NE3 sample using CT, the R_p value was simulated with Novalis Tx. After the CT was taken,

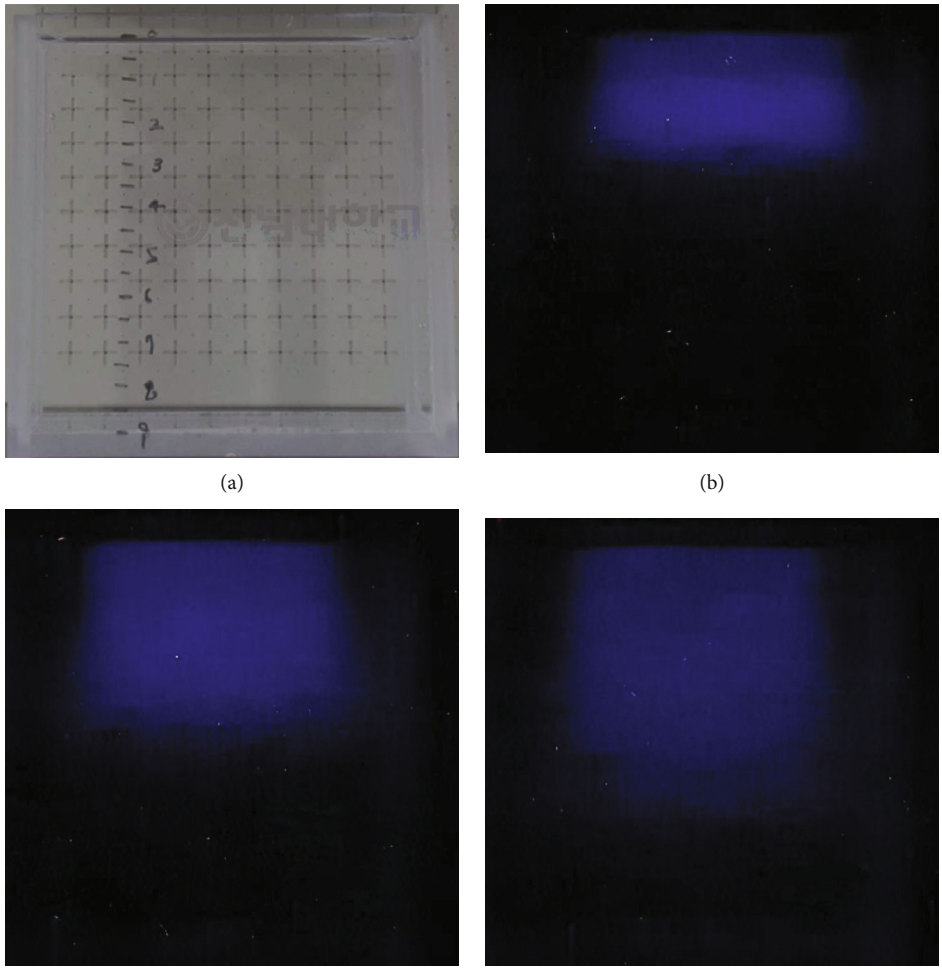

(a) (b)

(c) (d)

Figure 7: Range image of electron beam onto the NE3 sample: (a) acrylic container containing NE3 sample; (b) 6 MeV; (c) 9 MeV; (d) 12 MeV. These images were taken with the camera being exposed for 5 seconds when an electron beam is irradiated onto the sample. The electron beam generated from the Varian Novalis Tx system is injected from the top to the bottom of the container. If the V value in the HSV model is greater than 20%, only those pixels are selected, and their images are used to estimate the practical range.

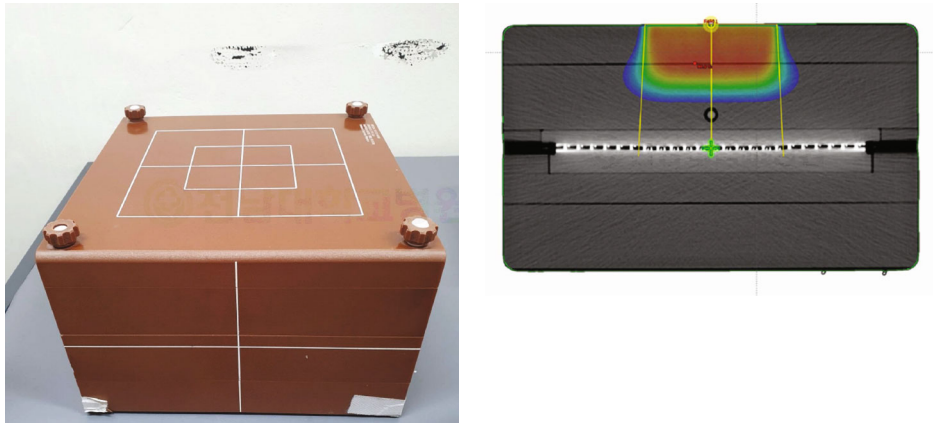

(a) (b)

Figure 8: (a) A water equivalent MapPHAN phantom. (b) Image of phantom with 12 MeV electron beam. The vertical yellow lines indicate the line of the cone used to prevent electron beams from spreading outward. The black circle represents ion-chamber position for measuring the absolute dose. When the brightest point on the image is set to 100, the distance to the point at which the brightness is 20% is selected to estimate a practical range. The color is arbitrary, and it is shown in rainbow-like color.

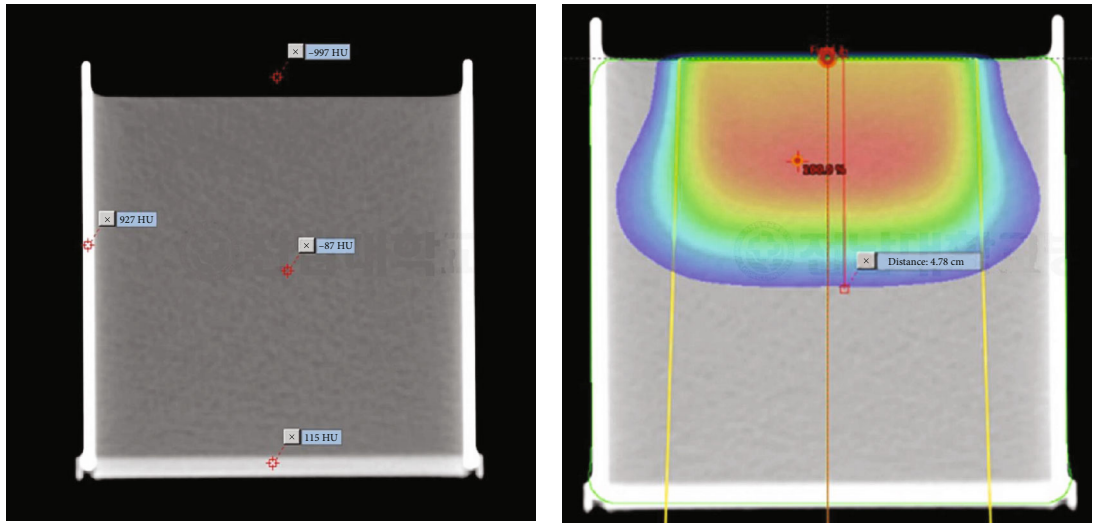

(a) (b)

Figure 9: (a) HU value of NE3 sample after taking General Electric CT image. (b) A simulated image of NE3 with 9 MeV electron beam from Varian Novalis Tx. The vertical yellow lines represent the line of the cone used to prevent electron beams from spreading outward.

the pixel values of the CT image are expressed in Hounsfield (HU) units, and then the HU can be converted to a given density with a known material type. A total of 4096 colors can be represented using 12 bits from black to white. The possible range is -1024 HU to 3071 HU including 0. For example, the air in the lungs represented as black with a value of -1024 HU, water is 0, and tooth enamel, the densest tissue in the human body, is white with a value of 3071 HU. Figure 9(a) shows the HU value when the CT of the NE3 sample was taken. The HU value of the LS was found to be -75, which is similar to that of fat. The HU value of fat is approximately -100. Figure 9(b) shows a simulated image of NE3 with a 9 MeV electron beam from Varian Novalis Tx being injected. The practical ranges were obtained using the same method applied in Figure 8. While changing the energy of the electron beam to 6, 9, or 12 MeV, the practical range values are 3.2, 4.8, and 6.4 cm, respectively.

4. Summary

A detection solution using alcohol as a new base material was developed for a liquid scintillator, and the possibility of using it for a particle detector was investigated. The basic physical and optical properties, such as transmittance, absorption, density, fluorescence, and pulse shape discrimination, were measured. The alcohol-based LS showed high transparency, and the energy exchange process between a solvent and fluor whereby the PPO absorption spectrum is overlapped with the bis-MSB emission spectrum can be seen in the alcohol-based LS. Light emission is possible by simply adjusting the composition ratio of the LS. As an example application of the alcohol-based LS, its use in medical physics was examined. A practical range measurement is introduced after irradiating an alcohol-based liquid scintillator with electron beam energies of 6~12 MeV. The results were compared and verified using several methods (Monte Carlo simulation, Novalis Tx, MapPHAN phantom, and CT image with Novalis Tx). There was no significant difference among these methods. In the future, this study could contribute to improving radiation treatment methods using an alcohol-based LS. Finally, in order for our alcohol-based LS to be used as a particle detector, it is necessary to be able to see Cherenkov radiation. Since the current samples are small, amounting to less than 100 ml, research should be conducted with larger size samples. At the same time, the ratio of alcohol to water should be minimized, and optimization studies on fluors and secondary WLS also should be performed. In this paper, we focused on the potential of an alcohol-based LS and several physical and optical properties are listed, but quantitative and systematic studies and longtime stability are required for use in future particle detectors.

Data Availability

All the data for our article can be found in the references.

Conflicts of Interest

The authors declare that there is no conflict of interests regarding the publication of this paper.

Acknowledgments

This work was supported by grants from National Research Foundation (NRF) of Korea (2019R1A2B5B01070451).

References

[1] W. Beriguete, J. Cao, Y. Ding et al., "Production of a gadolinium-loaded liquid scintillator for the Daya Bay reactor neutrino experiment," *Nuclear Instruments and Methods in Physics Research Section A*, vol. 763, pp. 82–88, 2014.

[2] C. Aberle, C. Buck, B. Gramlich et al., "Large scale Gd-beta-diketonate based organic liquid scintillator production for antineutrino detection," *Journal of Instrumentation*, vol. 7, no. 6, article P06008, 2012.

[3] F. Suekane, T. Iwamoto, H. Ogawa, O. Tajima, H. Watanabe, and KamLAND RCNS Group, "An overview of the KamLAND 1-kiloton liquid scintillator," pp. 279–290, 2004, Conference: C03-11-17.1.

[4] The RENO collaboration, C. D. Shin, Z. Atif et al., "Observation of reactor antineutrino disappearance using delayed neutron capture on hydrogen at RENO," *Journal of High Energy Physics*, vol. 2020, no. 4, article 29, 2020.

[5] J. S. Park, S. Y. Kim, C. Rott et al., "Production and optical properties of liquid scintillator for the JSNS2experiment," *Journal of Instrumentation*, vol. 14, no. 9, article T09010, 2019.

[6] F. An, G. An, Q. An et al., "Neutrino physics with JUNO," *Journal of Physics G: Nuclear and Particle Physics*, vol. 43, no. 3, 2016.

[7] Hyper-Kamiokande Proto-Collaboration, K. Abe, K. Abe et al., "Hyper-Kamiokande design report," 2018, physics.ins-det, https://arxiv.org/abs/1805.04163.

[8] S. W. Kim, "Dose distribution of 100 MeV proton beams in KOMAC by using liquid organic scintillator," *Journal of Radiological Science and Technology*, vol. 40, no. 4, pp. 621–626, 2017.

[9] Y. S. Park, Y. M. Jang, and K. K. Joo, "Constructing experimental devices for half-ton synthesis of gadolinium-loaded liquid scintillator and its performance," *Review of Scientific Instruments*, vol. 89, no. 4, article 043302, 2018.

[10] B. R. Kim, B. Y. Han, E. J. Jeon et al., "Pulse shape discrimination capability of metal-loaded organic liquid scintillators for a short-baseline reactor neutrino experiment," *Physica Scripta*, vol. 90, no. 5, article 055302, 2015.

[11] S. H. So, K. K. Joo, B. R. Kim et al., "Development of a liquid scintillator using water for a next generation neutrino experiment," *Advances in High Energy Physics*, vol. 2014, Article ID 327184, 7 pages, 2014.

[12] J. S. Park, J. Lee, I. S. Yeo et al., "Production and optical properties of Gd-loaded liquid scintillator for the RENO neutrino detector," *Nuclear Instruments and Methods in Physics Research Section A*, vol. 707, pp. 45–53, 2013.

[13] F. Elisei, F. Gatti, A. Goretti et al., "Measurements of liquid scintillator properties for the Borexino detector," *Nuclear Instruments and Methods in Physics Research A*, vol. 400, no. 1, pp. 53–68, 1997.

[14] H. O. Back, M. Balata, G. Bellini et al., "Pulse-shape discrimination with the counting test facility," *Nuclear Instruments and Methods in Physics Research A*, vol. 584, no. 1, pp. 98–113, 2008.

[15] I. Lalya, A. Maghous, E. A. Marnouche et al., "Radiotherapy of prostate cancer using rapid arc: dosimetric study of Military Teaching Hospital Mohamed V, Morocco," *Journal of Nuclear Medicine & Radiation Therapy*, vol. 8, no. 5, 2017.

[16] M. Khan and J. P. Gibbons, *The Physics of Radiation Therapy*, 256, Fifth edition, 2014.

[17] A. Ozdemir, S.-P. Teng, D. G. Lindstrom, and D. W. Anderson, "Calculations for distributions in water for 10-MeV electrons," *Radiation Research*, vol. 101, no. 2, p. 213, 1985.

[18] W. S. Kang, "Field size and dose distribution of electron beam," *Journal of the Korean Radiological Society*, vol. 16, no. 2, p. 678, 1980.